Topological Flat Bands from Dipolar Spin Systems

N. Y. Yao,[1] C. R. Laumann,[1,2] A. V. Gorshkov,[3] S. D. Bennett,[1] E. Demler,[1] P. Zoller,[4] and M. D. Lukin[1]

[1]*Department of Physics, Harvard University, Cambridge, Massachusetts 02138, USA*
[2]*ITAMP, Harvard University, Cambridge, Massachusetts 02138, USA*
[3]*Institute for Quantum Information and Matter, California Institute of Technology, Pasadena, California 91125, USA*
[4]*Institute for Quantum Optics and Quantum Information of the Austrian Academy of Sciences, A-6020 Innsbruck, Austria*

(Received 18 July 2012; published 26 December 2012)

We propose and analyze a physical system that naturally admits two-dimensional topological nearly flat bands. Our approach utilizes an array of three-level dipoles (effective $S = 1$ spins) driven by inhomogeneous electromagnetic fields. The dipolar interactions produce arbitrary uniform background gauge fields for an effective collection of conserved hard-core bosons, namely, the dressed spin flips. These gauge fields result in topological band structures, whose band gap can be larger than the corresponding bandwidth. Exact diagonalization of the full interacting Hamiltonian at half-filling reveals the existence of superfluid, crystalline, and supersolid phases. An experimental realization using either ultracold polar molecules or spins in the solid state is considered.

DOI: 10.1103/PhysRevLett.109.266804 PACS numbers: 73.43.Cd, 05.30.Jp, 37.10.Jk, 71.10.Fd

Single-particle flat bands, where kinetic energy is quenched relative to the scale of interactions, are being actively explored in the quest for novel strongly correlated phases of matter [1–8]. Prompted by the analogy to Landau levels, recent efforts have focused on *topological* flat bands —lattice models in which the band structure also harbors a nontrivial Chern invariant. Seminal recent work has highlighted that certain classes of highly engineered two-dimensional tight binding models can indeed exhibit topological nearly flat bands [9–14]. However, the identification of a physical system whose microscopics naturally admit topological flat bands remains an outstanding challenge.

In this Letter, we demonstrate the emergence of synthetic gauge fields for an ensemble of interacting hard-core bosons—the effective spin flips of pinned, three-level dipoles in a two-dimensional lattice. Underlying these gauge fields are two key ingredients: spatially varying, elliptically polarized external (microwave or optical) fields break time-reversal symmetry, while anisotropic dipolar interactions induce orientation-dependent phases onto the hopping hard-core bosons. The combination of these effects naturally produces nontrivial Chern numbers in the band structure and, when tuned appropriately, results in the emergence of flat bands due to hopping interference. While we observe a variety of nontopological correlated many-body states here (ranging from conventional crystals to supersolids), interacting particles living in such a flat-band-kinetic environment are also leading candidates for the realization of fractional Chern insulators [1–8]. Our proposal describes a natural framework in which ultracold molecules may be used to probe the exotic features of such interacting topological insulators.

Let us consider a square lattice composed of fixed, three-state magnetic or electric dipoles placed in a static external field. Such an arrangement naturally arises in experimental systems ranging from ultracold polar molecules [15–21] and Rydberg atoms [22–24] to solid-state spins [25,26] and magnetic atoms [27]. As shown in Fig. 1, the dipoles occupy the $\{X, Y\}$ plane and couple via dipole-dipole interactions,

$$H_{dd} = \frac{1}{2}\sum_{i\neq j}\frac{\kappa}{R_{ij}^3}[\mathbf{d}_i\cdot\mathbf{d}_j - 3(\mathbf{d}_i\cdot\hat{\mathbf{R}}_{ij})(\mathbf{d}_j\cdot\hat{\mathbf{R}}_{ij})], \quad (1)$$

where κ is $1/4\pi\epsilon_0$ for electric dipoles or $\mu_0/4\pi$ for magnetic dipoles, and $\mathbf{R}_{ij}$ connects the dipoles $\mathbf{d}_i$ and $\mathbf{d}_j$. The three states of each dipole, which we label as $|0\rangle$, $|\pm 1\rangle$, are eigenvectors of the $\hat{z}$ component of (rotational or spin) angular momentum. We assume that the $|\pm 1\rangle$ states are degenerate while the $|0\rangle$ state is energetically separated from them [Fig. 2(a)].

Each three-level dipole is driven by electromagnetic fields of Rabi frequency Ω_+ (right-circularly polarized), Ω_- (left-circularly polarized), and detuning Δ as shown

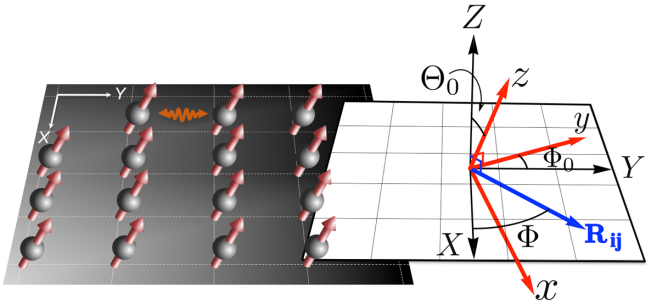

FIG. 1 (color online). Schematic representation of a 2D dipolar droplet. The grey droplet represents a 2D array of interacting tilted dipoles. The dipoles are tilted by a static field in the $\hat{z}$ direction, oriented at Θ_0, Φ_0 relative to the lattice basis $\{X, Y, Z\}$. $\mathbf{R}_{ij}$ is a vector connecting dipoles in the XY plane.

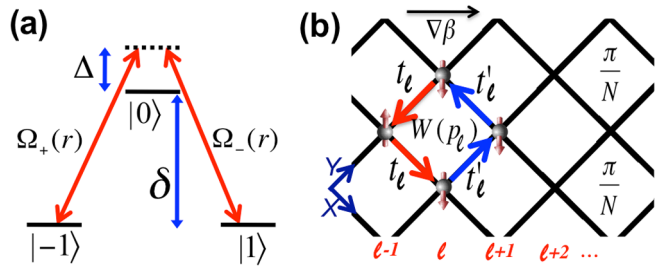

FIG. 2 (color online). (a) Depicts the on-site level structure and the two-photon driving scheme. These levels could, for example, be adiabatically connected to the $J = 1$ manifold of a rigid rotor as one turns on a dc electric field [see Eq. (6)]. The resonance frequency of the dressing lasers is detuned by Δ, while their Rabi frequencies are $\Omega_-(r)$ and $\Omega_+(r)$. We consider $|\Omega_\pm| \ll \Delta$ to operate in the far-detuned limit. In the case of polar molecules, δ is the electric-field induced splitting within the $J = 1$ manifold, which we require to be larger than the typical dipolar interaction strength. (b) Square lattice with a single tilted dipole per vertex. We index columns of the lattice by ℓ and plaquettes by p_ℓ. For a particle traversing the edge of a single plaquette, there are two contributions t_ℓ and t'_ℓ to $W(p_\ell)$; each contribution occurs twice as represented by the red and blue colored arrows. A simple periodic gradient of β enables uniform π/N flux per plaquette.

schematically in Fig. 2(a). With $|\Omega_+|, |\Omega_-| \ll \Delta$, the approximate eigenstates (dressed states) are $|0\rangle$, $|B\rangle = \alpha(|-1\rangle + \beta|1\rangle)$, and $|D\rangle = \alpha^*(-\beta^*|-1\rangle + |1\rangle)$, where $\alpha = \Omega_+/\tilde{\Omega}$, $\alpha\beta = \Omega_-/\tilde{\Omega}$, and $\tilde{\Omega} = \sqrt{|\Omega_-|^2 + |\Omega_+|^2}$. The energies of these dressed states are $E_0 = -\tilde{\Omega}^2/\Delta$, $E_B = \Delta + \tilde{\Omega}^2/\Delta$, and $E_D = \Delta$, respectively. We let d represent the typical size of the dipole moment and R_0 be the nearest-neighbor lattice spacing; by ensuring that $\kappa d^2/R_0^3 \ll \tilde{\Omega}^2/\Delta$ and so long as we initially avoid populating $|D\rangle$, the system remains within the subspace locally spanned by $|0\rangle$ and $|B\rangle$ (note that one could also choose to work in the subspace spanned by $|0\rangle$ and $|D\rangle$).

Thus, it is natural to view $|B\rangle$ as representing an effective hard-core bosonic excitation (spin flip), while $|0\rangle$ represents the absence of such an excitation. Recasting this system in terms of operators $a_i^\dagger = |B\rangle\langle 0|_i$ ($n_i = a_i^\dagger a_i$) yields a 2D model of conserved hard-core lattice bosons,

$$H_B = -\sum_{ij} t_{ij} a_i^\dagger a_j + \frac{1}{2}\sum_{i\neq j} V_{ij} n_i n_j, \tag{2}$$

where we define the hopping $t_{ij} = -\langle B_i 0_j|H_{dd}|0_i B_j\rangle$, the on-site potential $t_{ii} = \sum_{j\neq i}(\langle 0_i 0_j|H_{dd}|0_i 0_j\rangle - \langle B_i 0_j|H_{dd}|B_i 0_j\rangle)$, and the interaction $V_{ij} = \langle B_i B_j|H_{dd}|B_i B_j\rangle + \langle 0_i 0_j|H_{dd}|0_i 0_j\rangle - \langle B_i 0_j|H_{dd}|B_i 0_j\rangle - \langle 0_i B_j|H_{dd}|0_i B_j\rangle$. The conservation of total boson number, $N_i = \sum_i a_i^\dagger a_i$, arises from the condition $\kappa d^2/R_0^3 \ll \Delta$, which ensures that particle-number nonconserving terms of H_{dd} are energetically disallowed.

The functional form of the effective hard-core bosonic Hamiltonian Eq. (2) arises for any system of pinned, three-level dipoles. The parameters in H_B are given by ($\kappa = 1$, $i \neq j$):

$$\begin{aligned} t_{ij} &= \frac{d_{01}^2}{R^3}\{\chi_i^\dagger(q_0 + \mathrm{Re}[q_2]\sigma^x + \mathrm{Im}[q_2]\sigma^y)\chi_j\}, \\ t_{ii} &= -\sum_{j\neq i} 2\frac{q_0}{R^3}[d^0 d_i^B - (d^0)^2], \\ V_{ij} &= 2\frac{q_0}{R^3}[d_i^B d_j^B - d^0 d_i^B - d^0 d_j^B + (d^0)^2], \end{aligned} \tag{3}$$

where d^0 (d^B) is the permanent $\hat{z}$-dipole moment of the $|0\rangle$ ($|B\rangle$) state, d_{01} is the transition dipole moment from $|1\rangle$ to $|0\rangle$ [28], $\chi_i = \alpha_i(1, \beta_i)^T$ is the normalized drive-spinor on site i, $q_0 = \frac{1}{2}[1 - 3\cos^2(\Phi - \Phi_0)\sin^2(\Theta_0)]$, $q_2 = -\frac{3}{2}[\cos(\Phi - \Phi_0)\cos\Theta_0 - i\sin(\Phi - \Phi_0)]^2$, $\vec{\sigma}$ are the Pauli matrices, and (R, Φ) is the separation $\mathbf{R}_{ij}$ in polar coordinates (Fig. 1). We have suppressed the explicit ij dependence of R, Φ, q_0, and q_2. While the form of d_i^B, and hence of interactions, depends on the underlying implementation, the single-particle band structures that can be achieved via driving are independent of such details [29].

Let us first explore these topological single-particle bands and illustrate the interplay between the driven breaking of time reversal and the anisotropic dipolar interaction. As a simple example, we demonstrate how to achieve a synthetic background gauge field with uniform flux π/N per plaquette on a square lattice (assuming only nearest-neighbor hops). We choose the "magic" electric field tilt, $(\Theta_0, \Phi_0) = [\sin^{-1}(\sqrt{2/3}), \pi/4]$, where $q_0 = 0$ along $\hat{X}$ and $\hat{Y}$. This choice allows us to isolate the terms of H_{dd} that harbor intrinsic phases, namely, those associated with $d_i^+ d_j^+$ and $d_i^- d_j^-$, where $d_\pm = \mp(d_x \pm i d_y)/\sqrt{2}$ [18,28]. Moreover, it simplifies the form of nearest-neighbor hopping to

$$\begin{aligned} t_{ij}^{\hat{X}} &= \frac{d_{01}^2}{R_0^3}\chi_i^\dagger\left[\frac{1}{2}\sigma^x - \frac{\sqrt{3}}{2}\sigma^y\right]\chi_j, \\ t_{ij}^{\hat{Y}} &= \frac{d_{01}^2}{R_0^3}\chi_i^\dagger\left[\frac{1}{2}\sigma^x + \frac{\sqrt{3}}{2}\sigma^y\right]\chi_j. \end{aligned} \tag{4}$$

The microscopic breaking of time reversal arises from the asymmetry between left- and right-circularly polarized radiation and is captured by the ratio $\beta = \Omega_-/\Omega_+$. While each Rabi frequency is characterized by both an amplitude (intensity) and a phase, initially, we will consider only varying the amplitude of β; phase variations will be considered in more detail in the discussion of many-body states. Physically, it is β which defines each hard-core boson $|B\rangle$, by setting the relative admixture between the $|1\rangle$ and $|-1\rangle$ states. Keeping β real, let us now consider varying the intensities of the drive fields along the $\Phi = \pi/4$ direction in a periodic fashion.

For each plaquette, we define the Wilson loop, $W(p) = \prod_{\partial p} t_{ij}$, which is identical along columns indexed by ℓ [Fig. 2(b)]. The flux in a plaquette is then the phase of

this Wilson loop, $\Psi_\ell = \arg[W(p_\ell)] = \arg[t_\ell^2 t_\ell'^2]$, where t_ℓ and t_ℓ' are the hops depicted in Fig. 2(b). Taking $\theta_\ell = \arg(t_\ell)$ and noting that $\theta_\ell' = \arg(t_\ell') = -\theta_{\ell+1}$ yields the phase of the Wilson loop as $\Psi_\ell = 2\theta_\ell - 2\theta_{\ell+1}$. To achieve a uniform π/N flux per plaquette, we can take $\theta_{\ell+1} = \eta - \ell\frac{\pi}{2N}$, where $\eta \in \mathbb{R}$ is a constant to be specified. From the definition of θ_ℓ, one finds a simple recursion relation for β,

$$\frac{\beta_{\ell+1}}{\beta_\ell} = \frac{\sin(\frac{\pi}{3} - \eta + \ell\frac{\pi}{2N})}{\sin(\frac{\pi}{3} + \eta - \ell\frac{\pi}{2N})}, \tag{5}$$

with maximum periodicity $4N$ [30]. Starting from any initial β_1, Eq. (5) yields a recursively generated drive pattern which achieves the desired uniform π/N background gauge field.

While the uniform flux per plaquette is reminiscent of the square lattice Hofstadter problem [31], we emphasize that the physics of these driven dipoles is significantly richer, owing to the additional modulation of t_{ij}. The background flux field arises, in part, from the natural phases associated with the dipolar interaction. This ensures that (as in Ref. [32]) the number of flux quanta per plaquette is not limited by the magnitude of laser intensities, contrasting with the majority of previous synthetic gauge field proposals, where the scaling to high artificial fluxes is extremely difficult [33–37].

To illustrate the symmetry breaking required for the generation of gapped Chern bands, we now turn to a detailed study of H_B restricted to a two-site unit cell (remaining at the "magic" tilt), as depicted in Fig. 3(a). This restriction has the virtue of being analytically tractable and allows us to identify the antiunitary symmetries associated with the Dirac points [38,39]. Let us consider $\beta = \beta_1, \beta_2$ on the two sites of the unit cell and include all

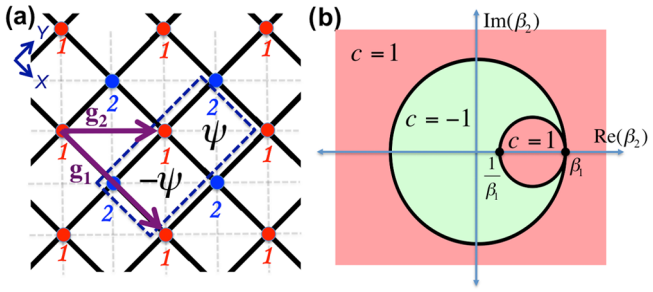

FIG. 3 (color online). (a) Schematic representation of the two-site unit cell lattice with $\beta = \beta_1, \beta_2$. The dotted box outlines a single unit cell. There is a flux Ψ, $-\Psi$ which alternates in neighboring square plaquettes. The direct lattice vectors g_1 and g_2 are depicted as purple arrows. While all hops are present with amplitude decaying as $1/R^3$, only nearest-neighbor (solid) and next-nearest-neighbor (dashed) hops are shown. (b) The topology of bulk bands as a function of complex β_2 for $\beta_1 \in \mathbb{R}$. The Chern number is $c = \frac{1}{4\pi}\int dk_x dk_y (\partial_{k_x}\hat{d} \times \partial_{k_y}\hat{d}) \cdot \hat{d}$, where $H(k) = \vec{d}(k) \cdot \vec{\sigma} + f(k)$.

terms up to next-next-nearest neighbor. The topology of the bands depends on the relative ratio of β_1 and β_2. For $\beta_1 \in \mathbb{R}$, the phase diagram in Fig. 3(b) illustrates the Chern invariant of the bottom band as a function of the complex β_2 plane. There exist two circles of gapless (Dirac) points protected by distinct antiunitary symmetries.

Implementation.—An experimental realization of our proposal can be envisioned with either electric (e.g., polar molecules) or magnetic (e.g., solid-state spins) dipoles. As previously mentioned, the form of d_i^B depends on this choice, since the permanent dipole moment of the $|\pm 1\rangle$ states have either the same or opposite signs. We emphasize that the long intrinsic lifetimes of such systems make them ideal for the consideration of driven, nonequilibrium phenomena [40,41].

To be specific, we now focus on diatomic polar molecules (trapped in a deep optical lattice) in their electronic and vibrational ground state. We utilize microwave fields to dress the molecules and partially polarize them with an applied dc electric field along $\hat{z}$ (Fig. 1); ignoring electronic and nuclear spins, this yields a single-molecule Hamiltonian,

$$H_m = BJ^2 - d_z E + H_D, \tag{6}$$

where B is the rotational constant, J is the rotational angular momentum operator, d_z is the $\hat{z}$ component of the dipole operator, E is the magnitude of the applied dc field, and H_D characterizes the dressing of the $J = 1$ rotational states depicted in Fig. 2(a) [18,40].

In the absence of applied fields, each molecule possesses rigid rotor eigenstates $|J, M\rangle$. The applied electric field $\mathbf{E}$ mixes eigenstates with the same M, splitting the degeneracy within each J manifold and inducing a finite dipole moment for each perturbed rotational state. We choose from among these states to form the effective three-level dipole; an example of one possibility for $|0\rangle$, $|\pm 1\rangle$ is shown in Fig. 2(a). Since these $|\pm 1\rangle$ states have an identical induced dipole moment d^1, one finds that $d_i^B = d^1$, and hence,

$$V_{ij} = 2\frac{q_0}{R^3}(d^0 - d^1)^2. \tag{7}$$

The relative strength of the interaction V_{ij}/t_{ij} is thus set by $(d^0 - d^1)^2/d_{01}^2$; this is a highly tunable parameter and can easily reach $\sim$100 for certain choices of rotational states and dc electric field strengths [18].

The main challenge in an experimental realization of our proposal lies in the spatial modulation of the drive fields at lattice scale. For spins in the solid-state and on-chip polar molecule experiments, one might envision using near-field techniques. A more straightforward approach, suitable for molecules, is to utilize pairs of optical Raman beams [42] (see Supplemental Material for details [30]). For example, the so-called lin $\perp$ lin configuration [43]

automatically ensures that $\tilde{\Omega}$ and Δ are identical on all sites and moreover, generically produces gapped topological band structures.

Many-body phases.—To illustrate the power of the present approach, we briefly explore two examples of correlated ground-state phases which arise in the Hamiltonian Eq. (2). As H_B conserves boson number N, we may consider its many-body physics at finite filling fractions ν (particle number per unit cell). Let us work with a two-site unit cell and truncate the dipolar interactions at next-next-nearest neighbor order. Bosons residing in a strongly dispersing band structure generically form superfluids in order to minimize their kinetic energy. Interaction dominated phases arise when the single-particle bands disperse less than the scale of interactions. Numerical optimization of the flatness ratio (band gap to lowest bandwidth) over the six-dimensional parameter space of microwave driving and tilt angle reveals approximately flat Chern bands in several regions of phase space. The flatness of these bands [Fig. 4(a)] derives from interference between the hopping in different directions and, microscopically, owes to an interplay between the natural anisotropy associated with dipolar interactions and the spatial variation of the drive fields.

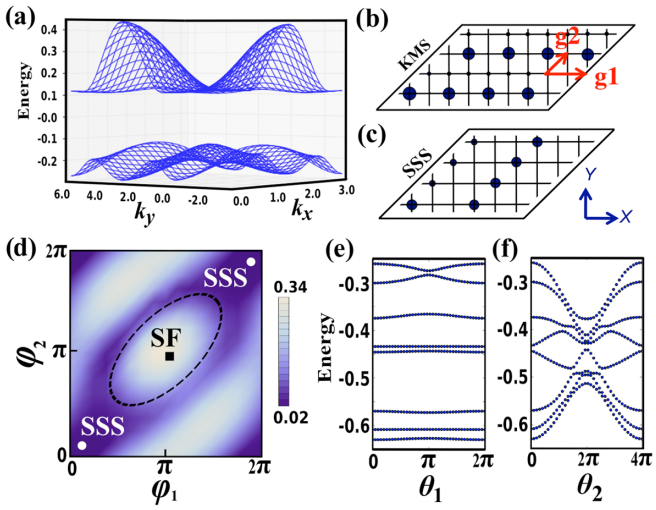

FIG. 4 (color online). Phase transitions in topological flat bands of 2D driven dipoles. (a) Band structure for $(\Theta_0, \Phi_0) = (0.46, 0.42)$, $\beta_1 = 3.6e^{2.69i}$, and $\beta_2 = 5.8e^{5.63i}$. We have verified that the Chern number does not change upon adding in dipolar interactions up to order $1/27R_0$. Significantly flatter band structures with a flatness ratio >10 can be obtained for slightly generalized configurations involving a tripod level structure and optical superlattice [42]. (b) Structure factor $S(R, 0) = \langle n(R)n(0)\rangle$ for filling $\nu = 1/2$ in KMS [30] and (c) SSS regime; size of circles indicates weight. (d) Spectral gap density plot as a function of varying microwave drive for parameters: $(\Theta_0, \Phi_0) = (0.66, \pi/4)$, $\beta_1 = -2.82e^{i\phi_1}$, $\beta_2 = -4.84e^{-i\phi_2}$, and $(d^0 - d^1)^2/d_{01}^2 \approx 2.8$. The transition from the SF, which has a unique finite-size ground state, to the degenerate SSS shows as a collapse of this gap. (e) Spectral flow in the ground state momentum sector of the SSS under twisting of the boson boundary condition in the $\hat{g}_1$ and (f) $\hat{g}_2$ directions. For the $N_s = 24$ lattice with 6 bosons, momentum sectors return to themselves after 2π in θ_1 and after 4π in θ_2.

As a first example, we consider the band structure depicted in Fig. 4(a), where the lower and upper band carry Chern index, $c = \mp 1$ (parameters in caption). Exact diagonalization at filling fraction $\nu = 1/2$ and relative interaction strength $(d^0 - d^1)^2/d_{01}^2 \approx 6$ reveals a knight's move solid (KMS) phase with a fourfold degenerate, gapped, ground state. The real-space structure factor $S(R, 0) = \langle n(R)n(0)\rangle$ (at total number of sites, $N_s = 32$) in Fig. 4(b) illustrates the knight's move relationship of the bosons in the ground state. Twisting the boundary condition of the KMS in the $\hat{g}_1$, $\hat{g}_2$ directions [Fig. 4(b)] does not significantly affect the ground-state energy, as expected of an insulator [30].

Many other commensurate phases arise as we tune the driving fields to other regions of phase space. Figure 4(d) shows a phase diagram containing both superfluid (SF) and striped supersolid (SSS) phases. We can characterize the SSS phase arising at $\phi_1 = \phi_2 = 0.1$ as follows: First, diagonalization reveals the existence of three degenerate ground states in the sectors: $k_2 = 0$, $k_1 = 0, 2\pi/3, 4\pi/3$. Consistent with striped ordering, the structure factor shows density stripes in the $\hat{g}_2$ direction [Fig. 4(c)]. However, each of these stripes has an incommensurate boson number, suggesting delocalization along the stripes. To wit, for $N_s = 24$, the 6 hard-core bosons are distributed evenly along two stripes, each containing four sites. Strong phase coherence along the stripes shows up in the sensitivity to twists in the $\hat{g}_2$ direction, while transverse twists produce essentially no dispersion, as shown in Figs. 4(e) and 4(f).

Conclusion.—Our proposal opens the door to a number of intriguing directions. In particular, the adiabatic preparation and detection of single-excitation states may provide an elegant approach to probing chiral dynamics, edge modes, and the Chern index [42,44,45]. More generally, dynamical preparation, manipulation and detection of many-body states in such driven topological systems remains an exciting open question [46]. Finally, the large available parameter space holds the promise of more exotic phases, such as fractional Chern insulators [42]. Realizing such phases in an effective spin system [47,48] may provide a deeper understanding of the stability of such states in the context of generalized long-range dipolar interactions.

We gratefully acknowledge conversations with A. Zhai, B. Lev, J. Preskill, J. Alicea, and N. Lindner. This work was supported, in part, by the NSF, DOE (FG02-97ER25308), CUA, DARPA, AFOSR MURI, NIST, Lawrence Golub Fellowship, Lee A. DuBridge Foundation, IQIM, and the Gordon and Betty Moore Foundation.

[1] R. Roy and S. L. Sondhi, Physics **4**, 46 (2011).
[2] N. Regnault and B. A. Bernevig, Phys. Rev. X **1**, 021014 (2011).
[3] G. Moller and N. R. Cooper, Phys. Rev. Lett. **108**, 045306 (2012).
[4] D. N. Sheng, Z.-C. Gu, K. Sun, and L. Sheng, Nat. Commun. **2**, 389 (2011).
[5] S. A. Parameswaran, R. Roy, and S. L. Sondhi, Phys. Rev. B **85**, 241308(R) (2012).
[6] Z. Liu, E. J. Bergholtz, H. Fan, and A. M. Laeuchli, Phys. Rev. Lett. **109**, 186805 (2012).
[7] Y.-F. Wang, Z.-C. Gu, C. De Gong, and D. Sheng, Phys. Rev. Lett. **107**, 146803 (2011).
[8] J. McGreevy, B. Swingle, and K.-A. Tran, Phys. Rev. B **85**, 125105 (2012).
[9] K. Sun, Z. Gu, H. Katsura, and S. D. Sarma, Phys. Rev. Lett. **106**, 236803 (2011).
[10] E. Tang, J.-W. Mei, and X.-G. Wen, Phys. Rev. Lett. **106**, 236802 (2011).
[11] T. Neupert, L. Santos, C. Chamon, and C. Mudry, Phys. Rev. Lett. **106**, 236804 (2011).
[12] M. Trescher and E. J. Bergholtz, arXiv:1205.2245v2.
[13] S. Yang, Z.-C. Gu, K. Sun, and S. D. Sarma, arXiv:1205.5792v1.
[14] Y.-F. Wang, H. Yao, C.-D. Gong, and D. N. Sheng, Phys. Rev. B **86**, 201101(R) (2012).
[15] A. Micheli, G. K. Brennen, and P. Zoller, Nat. Phys. **2**, 341 (2006).
[16] A. Micheli, G. Pupillo, H. P. Buchler, and P. Zoller, Phys. Rev. A **76**, 043604 (2007).
[17] J. Aldegunde, B. A. Rivington, P. S. Zuchowski, and J. M. Hutson, Phys. Rev. A **78**, 033434 (2008).
[18] A. V. Gorshkov, S. Manmana, G. Chen, E. Demler, M. Lukin, and A. M. Rey, Phys. Rev. A **84**, 033619 (2011); A. V. Gorshkov, S. Manmana, G. Chen, J. Ye, E. Demler, M. Lukin, and A. Rey, Phys. Rev. Lett. **107**, 115301 (2011).
[19] A. Chotia, B. Neyenhuis, S. Moses, B. Yan, J. Covey, M. Foss-Feig, A. Rey, D. Jin, and J. Ye, Phys. Rev. Lett. **108**, 080405 (2012).
[20] K. Aikawa, D. Akamatsu, M. Hayashi, K. Oasa, J. Kobayashi, P. Naidon, T. Kishimoto, M. Ueda, and S. Inouye, Phys. Rev. Lett. **105**, 203001 (2010).
[21] J. Deiglmayr, A. Grochola, M. Repp, K. Mörtlbauer, C. Glück, J. Lange, O. Dulieu, R. Wester, and M. Weidemüller, Phys. Rev. Lett. **101**, 133004 (2008).
[22] H. Schempp, G. Günter, C. S. Hofmann, C. Giese, S. D. Saliba, B. D. DePaola, T. Amthor, and M. Weidemüller, Phys. Rev. Lett. **104**, 173602 (2010).
[23] J. D. Pritchard, D. Maxwell, A. Gauguet, K. Weatherill, M. Jones, and C. Adams, Phys. Rev. Lett. **105**, 193603 (2010).
[24] L. Tagliacozzo, A. Celi, A. Zamora, and M. Lewenstein, arXiv:1205.0496v1.
[25] L. Childress, M. V. G. Dutt, J. M. Taylor, A. S. Zibrov, F. Jelezko, J. Wrachtrup, P. R. Hemmer, and M. D. Lukin, Science **314**, 281 (2006).
[26] G. Balasubramanian *et al.*, Nat. Mater. **8**, 383 (2009).
[27] M. Lu, S.-H. Youn, and B. L. Lev, Phys. Rev. Lett. **104**, 063001 (2010).
[28] We take $d^0 = \langle 0|d_z|0\rangle$, $d^B = \langle B|d_z|B\rangle$, and $d_{01} = \langle 0|d_-|1\rangle = -\langle -1|d_-|0\rangle \in \mathbb{R}$.
[29] The potential t_{ii} for each site is independent of i for polar molecules on a square lattice (since $d_i^B = d^1$) and for NV centers generally (since $d^0 = 0$). Alternatively, such an on-site potential can be corrected using a spatially dependent Stark shift.
[30] See Supplemental Material at http://link.aps.org/supplemental/10.1103/PhysRevLett.109.266804 for methods and theoretical derivations.
[31] D. R. Hofstadter, Phys. Rev. B **14**, 2239 (1976).
[32] N. R. Cooper, Phys. Rev. Lett. **106**, 175301 (2011).
[33] Y.-J. Lin, R. L. Compton, K. Jimnez-Garca, W. D. Phillips, J. V. Porto, and I. B. Spielman, Nature (London) **462**, 628 (2009).
[34] G. Juzeliunas, J. Ruseckas, P. Ohberg, and M. Fleischhauer, Phys. Rev. A **73**, 025602 (2006).
[35] J. R. Abo-Shaeer, C. Raman, J. M. Vogels, and W. Ketterle, Science **292**, 476 (2001).
[36] J. Dalibard, F. Gerbier, G. Juzeliūnas, and P. Öhberg, Rev. Mod. Phys. **83**, 1523 (2011).
[37] I. B. Spielman, Phys. Rev. A **79**, 063613 (2009).
[38] Y. Hatsugai, Phys. Rev. Lett. **71**, 3697 (1993).
[39] D. J. Thouless, M. Kohmoto, M. P. Nightingale, and M. den Nijs, Phys. Rev. Lett. **49**, 405 (1982).
[40] J. M. Brown and A. Carrington, *Rotational Spectroscopy of Diatomic Molecules* (Cambridge University Press, Cambridge, England, 2003).
[41] P. C. Maurer *et al.*, Science **336**, 1283 (2012).
[42] N. Y. Yao *et al.* (to be published).
[43] J. Dalibard and C. Cohen-Tannoudji, J. Opt. Soc. Am. B **6**, 2023 (1989); P. J. Ungar, D. S. Weiss, E. Riis, and S. Chu, *ibid.* **6**, 2058 (1989).
[44] N. Y. Yao *et al.*, arXiv:1110.3788v1.
[45] D. Abanin, T. Kitagawa, I. Bloch, and E. Demler (to be published).
[46] A. S. Sorensen, E. Altman, M. Gullans, J. V. Porto, M. D. Lukin, and E. Demler, Phys. Rev. A **81**, 061603(R) (2010).
[47] A. E. B. Nielsen, J. I. Cirac, G. Sierra, Phys. Rev. Lett. **108**, 257206 (2012).
[48] M. Greiter and R. Thomale, Phys. Rev. Lett. **102**, 207203 (2009).